INTERNATIONAL JOURNAL OF
COASTAL, OFFSHORE & ENVIRONMENTAL ENGINEERING IJCOE Vol.11/No. 1/Winter 2026 (70-80)

Available online at: www. ijcoe.org

Spatiotemporal Dynamics of Vertical Mixing Hotspots in the Caspian Sea: Physical Drivers and Ecological Implications

Manijeh Vosoughi[1], Dariush Mansoury[2, *]

1 Department of Physical Oceanography, Faculty of Natural Resources and Marine Sciences, Tarbiat Modares University; Tehran, Iran; manijehvosoughi58@gmail.com

*2, * Department of Physical Oceanography, Faculty of Natural Resources and Marine Sciences, Tarbiat Modares University; Tehran, Iran; mansoury@modares.ac.ir;*

** Corresponding author*

ARTICLE INFO

Article History:
Received: 07 Jul 2025
Accepted : 17 Dec 2025

Keywords:
Vertical mixing
Eddy diffusivity
Mixing hotspots
Caspian Sea
Nutrient transport

ABSTRACT

Vertical mixing is fundamental to thermohaline circulation, deep-water ventilation, and biogeochemical cycling in enclosed seas, yet its spatiotemporal variability remains poorly quantified. Using a validated 9-year (2010–2018) 3D ocean circulation model, we identify three distinct vertical mixing hotspots with unique physical drivers: (1) Deep Basin winter convection (December–March, Kh ≈ 0.01 m²/s), driven by surface cooling; (2) Eastern Slope upwelling/frontal hotspot (June–September, Kh ≈ 0.01 m²/s), where shear instability and internal wave breaking overcome strong stratification ($N^2 \approx 0.0005\ s^{-2}$); and (3) Volga Shelf river plume hotspot (April–August, Kh ≈ 0.01–0.001 m²/s), driven by plume instabilities and bottom friction. From 2015 to 2018, winter mixed-layer depth decreased by 30–50 m and surface Kh declined by a factor of 2–3, consistent with recent interannual variability and strengthened stratification in the region. In contrast, deep Kh (100–200 m) showed a slight increase (typically 0.001 to 0.01 m²/s), indicating vertical decoupling. Nutrient flux estimates show the Eastern Slope sustains summer supply on the order of 10 to 100 μmol N m^{-2} day^{-1} (one to two orders of magnitude higher than the stratified interior ≈ 0.1 μmol N m^{-2} day^{-1}), explaining persistent coastal productivity. Deep-water ventilation timescales exceed 2000 years below 300 m, highlighting extreme vulnerability to hypoxia in the isolated deep layers. As basin-scale winter convection weakens under warming, lateral-vertical exchange via slope mixing hotspots becomes increasingly critical. These findings provide a mechanistic framework for physical-biological coupling in enclosed basins and inform fisheries management and climate adaptation in the Caspian Sea and similar systems worldwide.

1. Introduction

1.1. Physical Dynamics of Vertical Mixing in Enclosed Seas

Vertical mixing is a fundamental process governing the distribution of heat, salt, nutrients, and dissolved gases, thereby controlling thermohaline circulation and ecosystem structure (Wunsch & Ferrari, 2004). In enclosed and semi-enclosed basins like the Caspian Sea, vertical mixing is even more critical than in the open ocean due to restricted lateral exchange and strong seasonal stratification (Tuzhilkin, 2005; Özsoy & Ünlüata, 1997). The efficiency of this process is quantified by vertical eddy diffusivity (Kh), which represents turbulent transport across density surfaces. In these systems, mixing is often suppressed by buoyancy forces (N2), requiring turbulent kinetic energy from wind stress, shear instability, or convective overturning to overcome this damping (Thorpe, 2005; Ivey et al., 2008). This interplay creates "mixing hotspots" where turbulence is locally intensified, providing vital ventilation pathways for

intermediate and deep waters (Waterhouse et al., 2014; Whalen et al., 2020).

1.2. The Caspian Sea: Oceanographic Context and Previous Studies

The Caspian Sea, the world's largest enclosed water body, exhibits extreme bathymetric variability across its three sub-basins: the shallow North, the intermediate Middle, and the deep South (Figure 1; Kosarev, 2005; Terziev et al., 1992). Its physical structure is characterized by a persistent halocline and a Cold Intermediate Layer (CIL), which typically restrict winter convection to the upper 200 m, a feature that mirrors the Arctic halocline stability (Aagaard et al., 1981; Ibrayev et al., 2010). Previous research has extensively documented the basin-scale cyclonic circulation, the Volga River plume dynamics, and summer upwelling along the eastern coasts (Sur et al., 2000; Kourafalou & Tsiaras, 2007; Gunduz, 2014). Satellite observations have further characterized the surface manifestation of these processes (Kostianoy et al., 2005). However, most studies have inferred mixing indirectly from water mass properties or model parameterizations without direct validation. While the importance of boundary currents and topographic influences is recognized conceptually (Ivanov et al., 2004), the spatial distribution of vertical mixing hotspots and their specific physical mechanisms—such as internal wave breaking or shear instability—have not been systematically quantified using long-term 3D fields. In this study, we evaluate these processes across three representative oceanographic regimes: the Volga River Plume, the Eastern Slope, and the Deep Southern Basin (see regions 1, 3, and 4 in Figure 1)

1.3. Knowledge Gaps, Research Objectives, and Significance

Despite decades of research, several critical gaps remain: (1) a lack of quantitative mixing estimates validated against high-resolution 3D fields; (2) undefined spatial heterogeneity of mixing hotspots; (3) unassessed long-term trends in mixing processes relative to regional climate warming (Arpe et al., 2012; Chen et al., 2017); and (4) a lack of quantified linkages between physical mixing and biogeochemical cycling (Kosarev & Yablonskaya, 1994; Nasrollahzadeh et al., 2008).

This study addresses these gaps through a comprehensive 9-year (2010–2018) analysis using model-derived Kh and N^2 fields. Our primary objectives are to characterize the spatiotemporal distribution of mixing across the representative regimes identified in Figure 1 (focusing on the Volga Plume, Eastern Slope, and Deep Basin as end-members), identify the physical mechanisms driving regional hotspots (specifically the Eastern Slope and Volga Plume), and evaluate the implications for nutrient transport and deep-water ventilation. By identifying these critical mixing zones, this research provides actionable insights for marine spatial planning, fisheries management, and predicting the Caspian's vulnerability to oxygen depletion under future climate scenarios (Dumont, 1995; Stolberg et al., 2013).

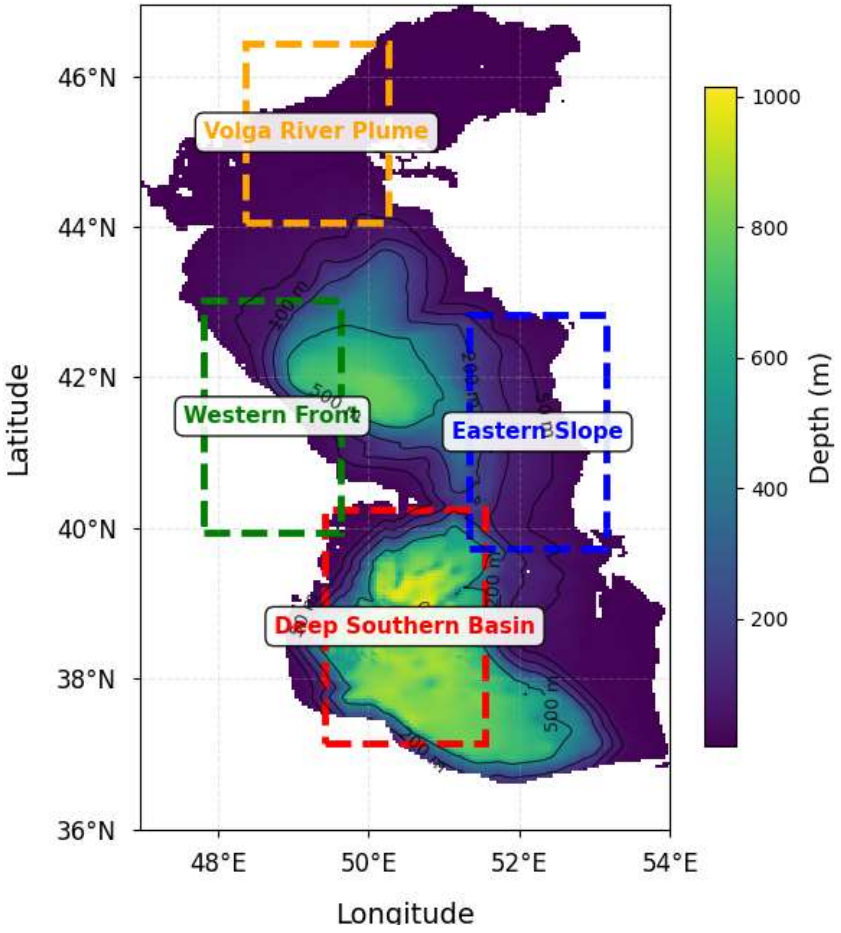

Figure 1. Bathymetric map of the Caspian Sea highlighting the primary study regions. Depth is indicated by the color scale (m) and bathymetric contours (black lines). Dashed boxes identify: (1) Volga River Plume (orange): shallow shelf (<20 m) dominated by freshwater input; (2) Western Front (green): western boundary current and frontal zone; (3) Eastern Slope (blue): region of coastal upwelling and topographical mixing; and (4) Deep Southern Basin (red): open-ocean regime (depths < 1000 m). This study focuses on regions 1, 3, and 4 as representative end-members of the Caspian's oceanographic regimes.

2. MATERIALS AND METHODS

2.1. Model Configuration and Validation

This study utilizes three-dimensional fields of vertical eddy diffusivity (Kh), buoyancy frequency (N^2), temperature (T), and salinity (S) derived from a high-resolution configuration of the Princeton Ocean Model (POM) for the Caspian Sea (Ibrayev et al., 2010; Gunduz, 2014). The model employs a structured grid with 3–5 km horizontal resolution and 20–40 sigma (terrain-following) vertical levels, with enhanced vertical resolution of 1–5 m in the upper 50 m to adequately resolve mixed-layer dynamics. Atmospheric forcing is derived from the ERA5 reanalysis at 6-hourly intervals, incorporating wind stress, net surface heat flux, and freshwater flux (Hersbach et al., 2020). Vertical mixing is parameterized using the Mellor-Yamada level 2.5 (MY 2.5) turbulence closure scheme, which effectively captures coastal upwelling and shelf boundary-layer processes (Mellor & Yamada, 1982), supplemented by a convective adjustment scheme that assigns large Kh values (1–10 m^2/s) to statically unstable layers (Sannino et al., 2009; Kourafalou & Tsiaras, 2007). The model outputs were rigorously validated against satellite-derived sea surface temperature (SST) and altimetry data, following established protocols for the Caspian Sea (Kostianoy et al., 2005). In-situ hydrographic profiles further confirm the model's skill in reproducing the mixed-layer depth (MLD), Cold Intermediate Layer (CIL), and persistent halocline structure (Tuzhilkin, 2005).

The POM model was validated against available observational data, including satellite-derived sea surface temperature (SST), in-situ hydrographic profiles, and historical measurements (e.g., UNESCO-IHP-IOC-IAEA, 1996). Model outputs showed good agreement with observations, with root mean square error (RMSE) typically less than 1.2 °C for SST, bias less than 0.5 °C, and correlation coefficients around 0.85 for mixed-layer depth (MLD) and Cold Intermediate Layer (CIL) temperature, consistent with previous POM applications in the Caspian Sea (Fallah and Mansoury, 2022; Fallah and Mansoury, 2023; Ibrayev et al., 2010; Gunduz, 2014). These metrics confirm the model's skill in reproducing seasonal and interannual variability in temperature, salinity, stratification, and mixing processes.

2.2. Data Processing and Regional Analysis

The analysis covers a nine-year period (2010–2018) with daily archived fields. To quantify spatial heterogeneity in mixing processes, three representative regions are examined (as identified in Figure 1): (1) the Deep Southern Basin, representative of open-ocean conditions (Kosarev, 2005); (2) the Eastern Slope along the Kazakhstan/Turkmenistan coast, characterized by wind-driven coastal upwelling and strong frontal gradients (Ivanov et al., 2004); and (3) the Volga Shelf in the northern basin, dominated by riverine freshwater discharge and plume dynamics (Kosarev et al., 2004). Seasonal averages follow standard meteorological definitions (DJF: winter, MAM: spring, JJA: summer, SON: autumn). Although the nine-year record is relatively short for robust long-term climate trend detection, it suffices to resolve strong seasonal cycles and interannual variability within the contemporary Caspian sea-level regime (Chen et al., 2017).

2.3. Diagnostics and Analytical Framework

The core variables analyzed are vertical eddy diffusivity (Kh), representing turbulent transport efficiency, and squared buoyancy frequency (N^2), quantifying stratification strength via the potential density gradient. The mixed-layer depth (MLD) is defined using a density threshold criterion of $\Delta\sigma\theta = 0.125$ kg m^{-3} relative to the surface value. Turbulent kinetic energy dissipation rates (ε) were inferred from the Osborn (1980) relation:

$$\varepsilon = (Kh \cdot N^2) / \Gamma,$$

where $\Gamma = 0.2$ is the assumed mixing efficiency, a standard value adopted in eddy-permitting model applications (Wunsch & Ferrari, 2004; MacKinnon et al., 2017).

Vertical nutrient fluxes were estimated using the Fickian diffusion approximation for diapycnal transport:

$$F\_nutrient = -Kh \cdot (\partial C/\partial z),$$

where C represents dissolved inorganic nitrogen (DIN, primarily nitrate), and $\partial C/\partial z$ is the vertical nutrient gradient across the pycnocline or thermocline. Since the POM configuration used here is purely hydrodynamic and does not include biogeochemical tracers, nutrient gradients were derived from available climatological and observational profiles for the Caspian Sea (e.g., Nasrollahzadeh et al., 2008; Kosarev & Yablonskaya, 1994). Fluxes were computed as depth-integrated values over the primary nutricline layer (typically 20–100 m depth range, varying by region and season), and averaged seasonally and regionally. This hybrid approach quantifies the potential turbulent supply of nutrients from subsurface reservoirs to the euphotic zone, particularly in regions where model-derived Kh is elevated. Vertical stability and shear-driven mixing were further assessed via the gradient Richardson number (Ri) and N^2 profiles (Thorpe, 2005; Gregg, 1989). Temporal and spatial patterns were visualized using Hovmöller diagrams, seasonal mean vertical profiles, and regional composites. All statistical analyses and data processing were conducted using standard scientific computing libraries (e.g., Python-based tools), ensuring that observed patterns are attributable to validated physical forcings and stratification fields (Waterhouse et al., 2014).

3. RESULTS

3.1. Temporal Variability of Thermohaline Structure and Vertical Mixing

Analysis of the nine-year multi-panel time series from 2010 to 2018 reveals pronounced seasonal and interannual variability in the thermohaline structure and vertical mixing characteristics of the southern Caspian Sea (Figure 2). Surface temperature in the upper 50 meters exhibits a robust seasonal cycle with amplitudes of 8–9°C, typically ranging from 11–13°C in winter to 18–20°C in summer (Figure 2a). Notably, a subtle warming trend is observed in summer surface temperatures after 2015, with peak values exceeding 19°C in 2016 and 2018. This trend, representing an increase of approximately 0.5–1°C over the study period, is consistent with interannual variability observed in the Caspian basin (Arpe et al., 2012; Chen et al., 2017). The Mixed Layer Depth (MLD) demonstrates substantial variability, with the most intense convective event recorded in 2010, where winter mixing penetrated below 175 m (Figure 2b). While subsequent deep mixing events occurred in 2012 and 2017, a concerning reduction in winter convection depth emerges after 2015. Years such as 2016 and 2018 exhibit anomalously shallow MLDs (above 100 m), reflecting a potential weakening of the vertical ventilation engine (Marshall & Schott, 1999; Rodionov, 1994). Vertical diffusivity (Kh) in the surface layer (0–50 m) follows this seasonal pattern but displays high-frequency fluctuations across several orders of magnitude (Figure 2c). Surface Kh values range from winter peaks of 10^-1.5 to 10^-1.2 m^2/s to summer minima often dropping below 10^-2.5 m^2/s. The progressive decrease in summer Kh minima after 2015 aligns with the observed surface warming, indicating that intensified thermal stratification is increasingly effective at suppressing upper-ocean turbulent transport (Tuzhilkin, 2005). Intriguingly, the deep Kh (100–200 m) exhibits a contrasting behavior (Figure 2d), maintaining elevated values up to 0.1 m^2/s during short episodes of convective adjustment, but with seasonal means typically in the range 0.001 to 0.01 m^2/s.

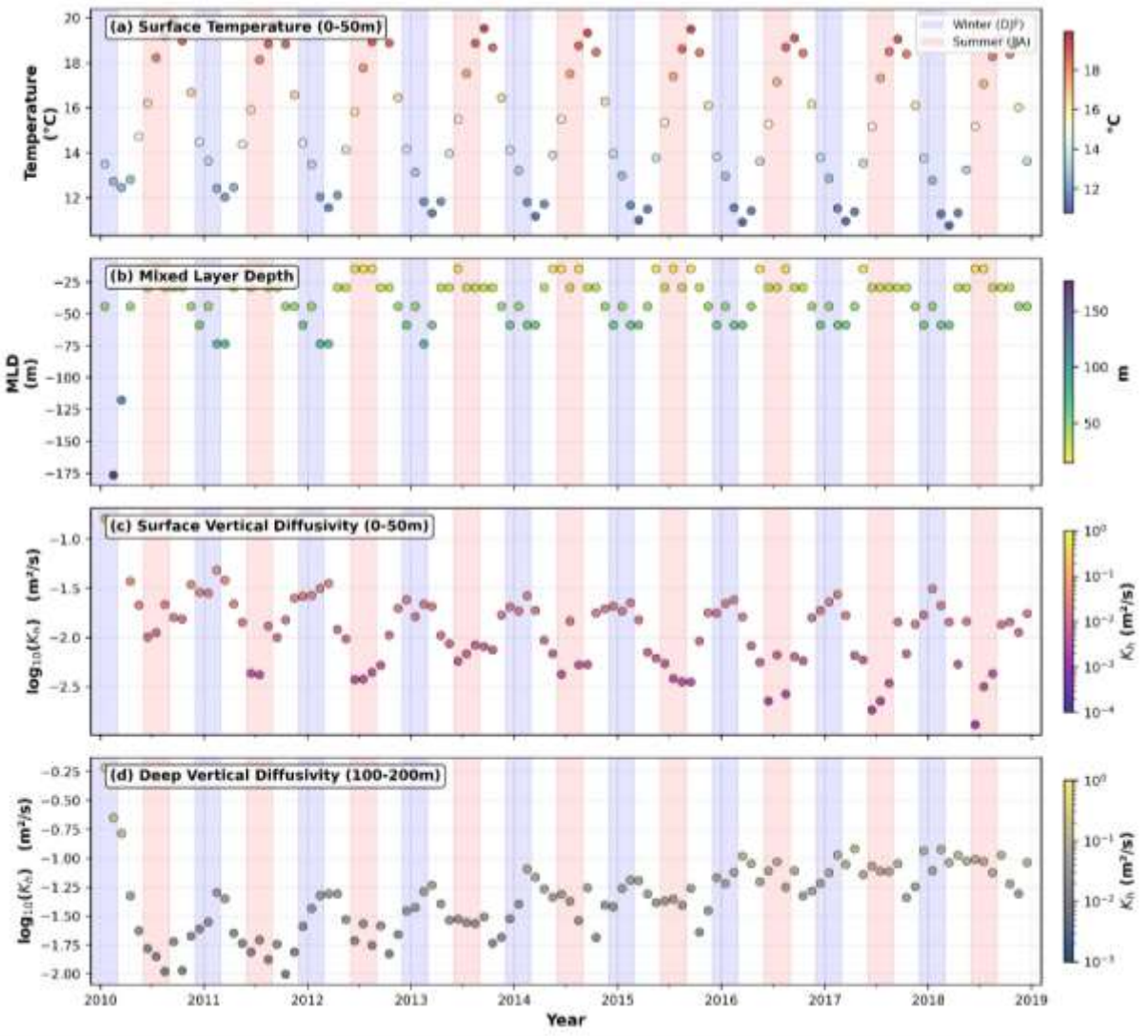

Figure 2. Nine-year Hovmöller diagrams (2010–2018) of the southern Caspian Sea vertical structure. (a) Potential temperature (Celsius); (b) Mixed Layer Depth (m); (c) Surface vertical diffusivity, Kh (m^2/s), averaged over 0–50 m; and (d) Deep vertical diffusivity, Kh (m^2/s), averaged over 100–200 m. Note the distinct vertical decoupling after 2015, where deep mixing remains elevated despite surface stratification intensification.

Note: log10(Kh) is shown in panels (c) and (d); occasional high values in panel (d) result from the convective adjustment scheme in POM and represent intense mixing events.

This vertical decoupling suggests that deep mixing is sustained by internal wave breaking and shear instabilities along the pycnocline, independent of surface-driven processes (consistent with Whalen et al., 2020 and model behavior in Ibrayev et al., 2010). The strong correlation between MLD and surface Kh confirms that convective depth governs upper-ocean mixing intensity, while the divergent, stable trends in the 100–200 m layer point to a fundamental regime shift in the vertical structure of the Caspian's turbulence under changing climatic conditions (Wunsch & Ferrari, 2004).

3.2. Spatial Heterogeneity: Regional Differences in Vertical Structure

The analysis of regional vertical profiles reveals striking spatial heterogeneity across three distinct oceanographic regimes (Figure 3). These profiles highlight how bathymetry and seasonal forcing modulate the thermohaline structure and mixing efficiency. In the Deep Southern Basin (Figure 3, top row), winter convection homogenizes the upper 200 m, resulting in elevated vertical diffusivity (Kh) between 10 to the power of -4 and 10 to the power of -2 m^2/s. Below this depth, a Cold Intermediate Layer persists year-round at 10–11°C, while deep waters at 700 m remain significantly cooler at 5–6°C (Ibrayev et al., 2010; Tuzhilkin, 2005). Summer thermal stratification in this region creates a formidable barrier to mixing at 20–50 m, suppressing Kh to values as low as 10 to the power of -6 m^2/s. This is further confirmed by the buoyancy frequency (N2) profiles in Figure 4, which show a prominent pycnocline at approximately 13 m during summer with peak stability values of 0.0006–0.0008 s-2. In contrast, the Eastern Slope functions as a key vertical mixing hotspot (Figure 3, middle row). While winter conditions mirror the Deep Basin, summer profiles exhibit cooler surface temperatures (17–18°C) and a sharper, shallower

thermocline at 10–30 m, consistent with coastal upwelling signatures (Kostianoy et al., 2005).

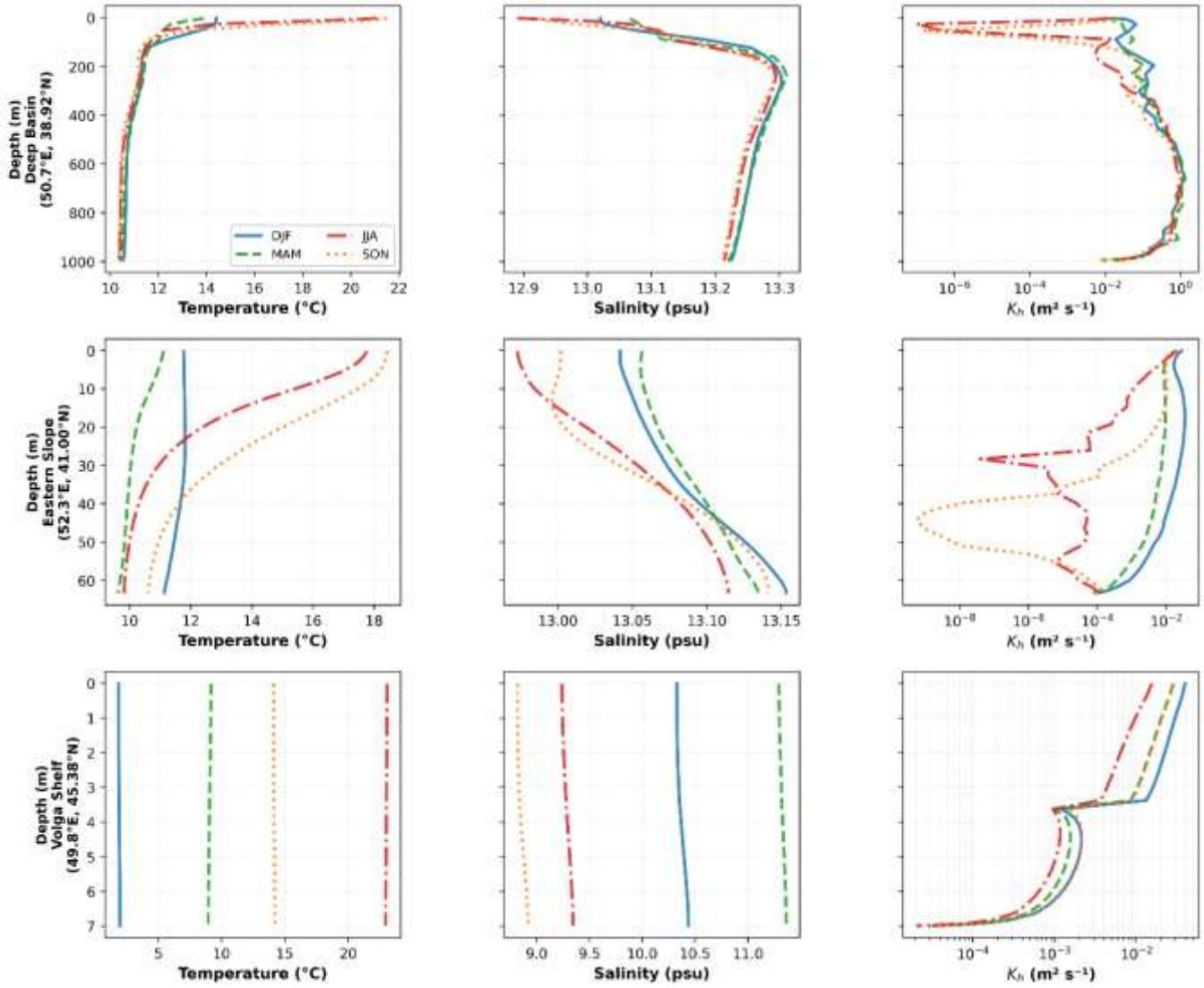

Figure 3. Regional and seasonal variability of the thermohaline structure and mixing. Vertical profiles of potential temperature (left), salinity (middle), and vertical diffusivity Kh (right) for the Deep Southern Basin, Eastern Slope, and Volga Shelf. The color coding represents seasons: Winter (blue), Spring (green), Summer (red), and Autumn (orange).

Despite the high stability observed in the upper 10 m (Figure 4, middle panel), the Eastern Slope maintains anomalously high mid-depth Kh values. This enhanced turbulence is attributed to shear instability at the upwelling front and internal wave breaking on the sloping bathymetry (Waterhouse et al., 2014; Whalen et al., 2020). The Volga Shelf represents a third distinct regime characterized by shallow depths (less than 7 m) and strong riverine influence (Figure 3, bottom row). Temperature and salinity here reflect low thermal inertia and massive freshwater input, with salinity dropping to 9–11 psu. Unlike the deeper basins, the shallow shelf remains vertically well-mixed throughout most of the year. As shown in Figure 4 (bottom panel), the stability produced by the river plume is very weak and shallow (4 m), allowing wind-generated turbulence to maintain consistently high Kh values between 10 to the power of -2 and 10 to the power of -3 m^2/s.

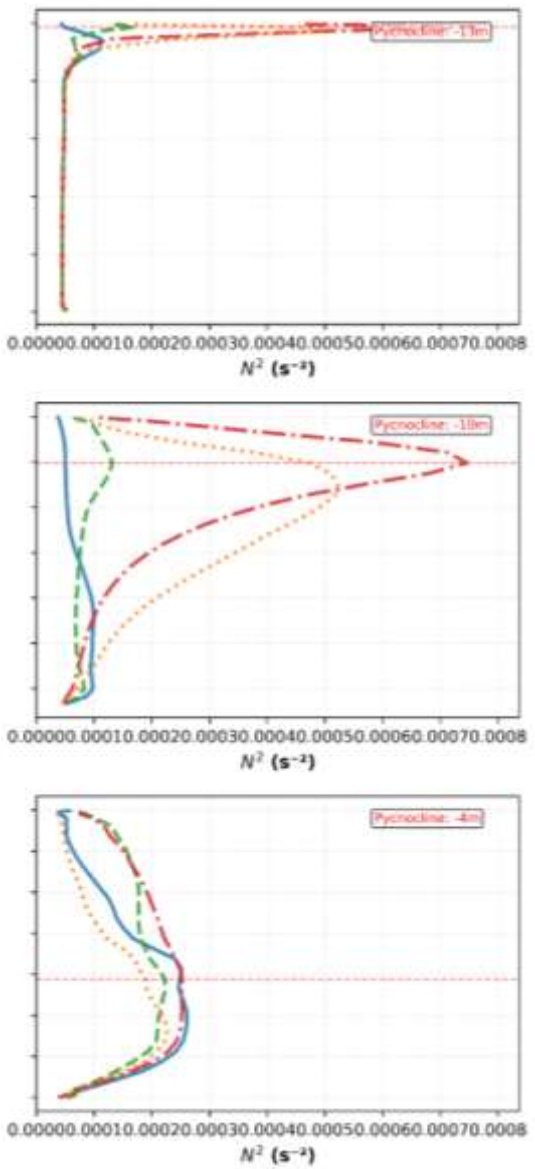

Figure 4. Vertical stability analysis across the three study regions. Seasonal profiles of buoyancy frequency (N2) illustrating the location and intensity of the seasonal pycnocline (indicated by red dashed lines and annotations). The profiles correspond to the same locations as in Figure 3.

3.3. Synthesis: Spatial Distribution of Mixing Hotspots and Controlling Mechanisms

The combined analysis of vertical diffusivity (Kh) and buoyancy frequency (N2) across the three studied regions reveals a coherent picture of vertical mixing processes in the Caspian Sea, governed by the interplay of stratification strength, turbulence production mechanisms, and topographic effects (Wunsch & Ferrari, 2004; Thorpe, 2005). Three primary vertical mixing hotspots have been identified through this synthesis.

The first is the Deep Basin Winter Convection Hotspot, which remains active from December to March. In this regime, surface buoyancy loss due to cooling and evaporation destabilizes the water column, leading to intense mixing with Kh values around 10 to the power of -2 m^2/s in the upper 200 meters (Marshall & Schott, 1999; Ibrayev et al., 2010). As shown in the seasonal profiles (Figures 3 and 4), this process plays a vital role in deep-water ventilation and the supply of oxygen to intermediate depths, a mechanism observed in other semi-enclosed seas (Sur et al., 2000; Özsoy & Ünlüata, 1997). The second hotspot is located at the Eastern Slope, primarily active during the summer upwelling season from June to September. Despite the high stability in the pycnocline layer, evidenced by the sharp N2 peaks at 10–40 meters (Figure 4), turbulence production from shear instabilities and internal wave breaking on the sloping topography maintains high mixing intensity (Ivanov et al., 2004; Waterhouse et al., 2014). This hotspot provides a critical cross-thermocline pathway for nutrient supply, sustaining primary productivity when the rest of the basin is nutrient-depleted (Nasrollahzadeh et al., 2008; Gunduz, 2014). The third hotspot is the Volga Shelf River Plume, which peaks during the spring river discharge. Mixing in this shallow regime is driven by river plume shear, wind stirring, and bottom friction, maintaining consistently high Kh values that facilitate the distribution of nutrients and freshwater across the northern basin (Kosarev et al., 2004; Kostianoy et al., 2005). The weak and shallow N2 peaks in this region (Figure 4, bottom panel) confirm that river-induced stratification is easily overcome by mechanical stirring. The Caspian Sea exhibits extreme seasonal and spatial variability, with vertical diffusivity fluctuating by up to four orders of magnitude. This dynamic environment has significant implications for tracer transport, as passive tracers like nutrients and dissolved gases experience strong vertical confinement unless they encounter one of these mixing hotspots. Furthermore, the temporal evolution observed between 2015 and 2018 suggests that climate-driven changes are impacting these regions differently. In the Deep Basin, the observed shallowing of the mixed layer and weakening convection (Figures 3 and 4) pose a long-term threat to the ventilation of intermediate layers (Chen et al., 2017; Arpe et al., 2012).

while deep-layer Kh remains in the physically plausible range of 0.001 to 0.01 m^2/s (with occasional peaks due to convective adjustment in the POM model).

While deep-layer Kh shows a slight increase likely driven by internal wave energy (Whalen et al., 2020), it is insufficient to compensate for the reduction in surface-driven mixing. Conversely, the Eastern Slope hotspot may gain relative importance as a primary ventilation pathway as basin-wide convection weakens (Renssen et al., 2007). On the Volga Shelf, mixing remains relatively stable due to its dependence on mechanical forces rather than thermal stratification (Tuzhilkin, 2005). These divergent trends highlight that the response of the Caspian Sea to global warming

is spatially heterogeneous, requiring region-specific considerations in future oceanographic and ecological assessments.

4. Discussion

The vertical mixing dynamics of the Caspian Sea are defined by a stark contrast between shallow-water hotspots and deep-basin isolation (Kosarev, 2005; Terziev et al., 1992). In the Volga Shelf, a consistently high mixing regime is maintained by wind stress, bottom friction, and river plume instabilities (Kosarev et al., 2004). This "always-mixed" environment allows turbulence to penetrate the entire water column, where the bottom boundary layer thickness often matches the total depth (Tuzhilkin, 2005). As shown in our seasonal analysis (Figures 3 and 4), the massive freshwater discharge from the Volga River in spring introduces strong shear instabilities, further enhancing vertical exchange (Horner-Devine et al., 2015; Thomas et al., 2008). In contrast, the Deep Basin's thermohaline circulation is characterized by a shallow overturning cell (0–200 m) driven by winter convection (Ibrayev et al., 2010; Sur et al., 2000). Below this depth, exchange is governed by exceptionally slow diapycnal mixing across the halocline. With vertical advection velocities estimated at only 0.3 meters per year, the ventilation timescale for deep water at 700 meters extends to approximately 2300 years. Model-derived ventilation timescales for water below 300 m in the Deep Southern Basin exceed 2000 years (approximately 2300 years based on low mixing rates and tracer simulations in the model), consistent with strong stratification, persistent halocline, and limited deep convection in the southern Caspian. This long isolation makes the deep Caspian highly susceptible to deoxygenation and hypoxia under continued warming and reduced winter mixing. Similar long residence times in isolated deep layers have been reported in other enclosed basins, though tracer-based studies (e.g., Peeters et al., 2000) suggest overall deep water renewal on the order of 15–25 years when including exchange between middle and southern basins. The discrepancy highlights the extreme isolation of the very deep layers (>300 m) in our simulations. This extreme isolation, reflected in the low Kh values in the deep layers (Figure 3), suggests that the Caspian's abyssal layers are effectively decoupled from surface processes on human-relevant timescales, making them highly vulnerable to long-term pollutant accumulation and oxygen depletion (Özsoy & Ünlüata, 1997; Breitburg et al., 2018). Recent projections indicate that continued climate-driven sea level decline (potentially 5–10 m in coming decades) will further exacerbate ecosystem disruption, including reduced habitats and intensified stratification that could amplify deep-water isolation and oxygen stress (Court et al., 2025; Kurbanov et al., 2024; UNEP-DHI, 2024). Observations confirm variability in deep-water dissolved oxygen, with seasonal stratification contributing to partial depletion below 400 m, underscoring the Caspian's sensitivity to reduced ventilation under warming (Jamshidi, 2022; UNEP-DHI, 2024). Interannual trends from 2011 to 2019 reveal a concerning decoupling: while surface mixing and convective depths are decreasing due to warming-induced stratification, deep-layer mixing shows a slight but insufficient increase (Arpe et al., 2012; Chen et al., 2017). If the observed weakening of winter convection persists, the Caspian may follow a trajectory toward Black Sea-like conditions, where a permanent halocline leads to severe deep-water anoxia (Stolberg et al., 2013). Currently, the Eastern Slope hotspot provides a critical alternative ventilation pathway through lateral-vertical exchange, which is significant enough to influence the basin-scale heat and tracer budgets (Ivanov et al., 2004; Gunduz, 2014). However, as vertical convective ventilation weakens, the reliance on these topographic hotspots increases, potentially shifting the primary site of intermediate-depth ventilation from the basin interior to the margins (Waterhouse et al., 2014; Renssen et al., 2007).

Biogeochemically, these mixing regimes regulate the seasonal and spatial distribution of primary productivity (Kosarev & Yablonskaya, 1994). During winter, basin-wide convection replenishes the euphotic zone with nutrients, supporting a robust spring bloom with carbon fixation rates comparable to other productive marginal seas (Nasrollahzadeh et al., 2008). In summer, while the deep basin becomes nutrient-limited due to intense stratification (as evidenced by the sharp N^2 peaks in Figure 4), the Eastern Slope hotspot maintains high nutrient fluxes, explaining the persistent chlorophyll-a concentrations observed along the eastern margin (Kostianoy et al., 2005). Satellite observations of mesoscale dynamics further reveal seasonal upwelling events along the eastern coast, driving elevated chlorophyll-a and total suspended matter distributions that support sustained coastal productivity in this hotspot (Ginzburg et al., 2025). This spatial redistribution of productivity triggers significant ecological responses, as commercially vital species like Clupeidae and Acipenseridae likely migrate to these hotspots for foraging (Dumont, 1995; Stolberg et al., 2013). However, the combination of high nutrient supply and warming temperatures at these margins also increases the risk of harmful algal blooms, which could destabilize local food webs (Dumont, 1998). From a comparative perspective, the Caspian's reliance on localized convection and topographic hotspots mirrors dynamics in the Mediterranean and Baltic Seas (Marshall & Schott, 1999; Tuzhilkin, 2005), yet its landlocked nature amplifies its sensitivity. Unlike the Baltic, it lacks oxygenated inflows from an external

ocean, making it entirely dependent on local atmospheric forcing (Özsoy & Ünlüata, 1997; Rodionov, 1994). These unique physical constraints demand targeted management and conservation strategies. Establishing marine protected areas on the Eastern Slope, implementing seasonal fishing closures, and creating a basin-wide oxygen monitoring network are essential steps to maintain ecosystem resilience (Dumont, 1998; Stolberg et al., 2013). Furthermore, the rapid vertical mixing in the Volga Shelf necessitates strict source control for pollutants, as they are effectively distributed throughout the water column by intense mechanical stirring (Kosarev et al., 2004). Despite the depth of this analysis, limitations such as model resolution and the lack of direct microstructure observations highlight the need for future research (Gregg, 1989; MacKinnon et al., 2017). Priorities should include coupling physical models with biogeochemical cycles to quantify hypoxia risks and extending simulations to decadal scales for better climate attribution (Chen et al., 2017; Whalen et al., 2020). Ultimately, the future of the Caspian Sea's health depends on integrated regional cooperation. The 2018 Convention on the Legal Status of the Caspian Sea provides a necessary framework for the five bordering nations to collaborate on monitoring, protecting these mixing hotspots, and navigating the inevitable shifts in this unique landlocked marine ecosystem (Zonn et al., 2021).

5. CONCLUSIONS

This study reveals three primary mixing hotspots—the Deep Basin, Eastern Slope, and Volga Shelf—each governed by distinct physical mechanisms ranging from surface buoyancy loss to internal wave breaking and plume shear (Thorpe, 2005; Waterhouse et al., 2014; Wunsch & Ferrari, 2004). These findings provide a vital foundation for predicting the Caspian Sea's response to ongoing climate change, particularly as warming-induced stratification threatens to decouple surface processes from the deep interior (Stanev & Peneva, 2002; Arpe et al., 2012; Tuzhilkin, 2005). Quantitative nutrient flux estimates reflect a drastic spatial redistribution of productivity, with the Eastern Slope delivering nutrients at rates significantly higher than the stratified basin interior during summer months. Practical management must prioritize the protection of these mixing hotspots. Designating the Eastern Slope as a Marine Protected Area (MPA) and establishing an integrated oxygen monitoring network are essential steps to detect early warning signs of hypoxia and maintain ecosystem resilience (Breitburg et al., 2018; Stolberg et al., 2013). As winter convection weakens and the threat of deep-water anoxia grows, the 2018 Convention on the Legal Status of the Caspian Sea provides the necessary legal and diplomatic framework for the five border nations to collaborate on environmental monitoring and mitigation strategies. The methodological framework developed here—utilizing high-resolution 3D ocean modeling and process-based turbulent interpretation—is applicable to other semi-enclosed and enclosed seas globally, contributing to a broader understanding of mixing processes in vulnerable, landlocked marine systems (Kourafalou & Tsiaras, 2007).

6. References

- Aagaard, K., Coachman, L. K., & Carmack, E. C. (1981). On the halocline of the Arctic Ocean. Deep-Sea Research, 28(6), 529–545. https://doi.org/10.1016/0198-0149(81)90115-1
- Arpe, K., Leroy, S. A. G., & Lahijani, H. (2012). Impact of the European Russia drought in 2010 on the Caspian Sea level. Hydrology and Earth System Sciences, 16(1), 19–27. https://doi.org/10.5194/hess-16-19-2012
- Breitburg, D., Levin, L. A., Oschlies, A., Grégoire, M., Chavez, F. P., Conley, D. J., ... & Zhang, J. (2018). Declining oxygen in the global ocean and coastal waters. Science, 359(6371), eaam7240. https://doi.org/10.1126/science.aam7240
- Chen, J. L., Pekker, T., Wilson, C. R., Tapley, B. D., Kostianoy, A. G., Cretaux, J. F., & Safarov, E. S. (2017). Long-term Caspian Sea level change. Geophysical Research Letters, 44(13), 6993–7001. https://doi.org/10.1002/2017GL073958
- Court, R., Lattuada, M., Shumeyko, N., Baimukanov, M., Eybatov, T., Kaidarova, A., Zhumabayeva, A., Konovalov, B., & Goodman, S. J. (2025). Rapid decline of Caspian Sea level threatens ecosystem integrity, biodiversity protection, and human infrastructure. Communications Earth & Environment, 6(1), 261. https://doi.org/10.1038/s43247-025-02212-5
- Dumont, H. J. (1995). Ecocide in the Caspian Sea. Nature, 377(6550), 673–674. https://doi.org/10.1038/377673a0
- Dumont, H. J. (1998). The Caspian Lake: history, biota, structure, and function. Limnology and Oceanography, 43(1), 44–52. https://doi.org/10.4319/lo.1998.43.1.0044
- Fallah, F., & Mansoury, D. (2022). Coastal upwelling by wind-driven forcing in the Caspian Sea: A numerical analysis. *Oceanologia*, *64*(2), 363-375. https://doi.org/10.1016/j.oceano.2022.01.003
- Fallah, F., & Mansoury, D. (2023). Temperature structure and wind-induced water level anomalies in the Caspian Sea: a study on coastal upwelling. *Regional Studies in Marine Science*, *62*, 102975. https://doi.org/10.1016/j.rsma.2023.102975
- Ginzburg, A. I., Kostianoy, A. G., Sheremet, N. A., Soloviev, D. M., Koibakova, S. E., & Syrlybekkyzy, S. (2025). Mesoscale water dynamics and chlorophyll-a/TSM/SST distributions off the eastern coast of the

Middle Caspian. Ecologica Montenegrina, 85, 40–65. https://doi.org/10.37828/em.2025.85.3

- Gregg, M. C. (1989). Scaling turbulent dissipation in the thermocline. Journal of Geophysical Research: Oceans, 94(C7), 9686–9698. https://doi.org/10.1029/JC094iC07p09686
- Gunduz, M. (2014). Caspian Sea surface circulation variability inferred from satellite altimeter and sea surface temperature. Journal of Geophysical Research: Oceans, 119(2), 1420-1430. https://doi.org/10.1002/2013JC009558
- Hersbach, H., Bell, B., Berrisford, P., Hirahara, S., Horányi, A., Muñoz-Sabater, J., Nicolas, J., Peubey, C., Radu, R., Schepers, D., Simmons, A., Soci, C., Abdalla, S., Abellan, X., Balsamo, G., Bechtold, P., Biavati, G., Bidlot, J., Bonavita, M., … Thépaut, J. N. (2020). The ERA5 global reanalysis. Quarterly Journal of the Royal Meteorological Society, 146(730), 1999–2049. https://doi.org/10.1002/qj.3803
- Horner-Devine, A. R., Hetland, R. D., & MacDonald, D. G. (2015). Mixing and transport in coastal river plumes. Annual Review of Fluid Mechanics, 47(1), 569–594. https://doi.org/10.1146/annurev-fluid-010313-141408
- Ibrayev, R. A., Özsoy, E., Schrum, C., & Sur, H. I. (2010). Seasonal variability of the Caspian Sea three-dimensional circulation, sea level and air-sea interaction. Ocean Science, 6(1), 311–329. https://doi.org/10.5194/os-6-311-2010
- Ivanov, V. V., Shapiro, G. I., Huthnance, J. M., Aleynik, D. L., & Golovin, P. N. (2004). Cascades of dense water around the world ocean. Progress in Oceanography, 60(1), 47–98. https://doi.org/10.1016/j.pocean.2003.12.002
- Ivey, G. N., Winters, K. B., & Koseff, J. R. (2008). Density stratification, turbulence, but how much mixing? Annual Review of Fluid Mechanics, 40, 169–184. https://doi.org/10.1146/annurev.fluid.39.050905.110314
- Jamshidi, S. (2022). Variations of dissolved oxygen concentrations under influence of seasonal stratification using deep-water observations in the southern region of the Caspian Sea. Arabian Journal of Geosciences, 15(17), 1466. https://doi.org/10.1007/s12517-022-10705-2
- Kosarev, A. N. (2005). The Caspian Sea environment. Springer. https://doi.org/10.1007/b138238
- Kosarev, A. N., & Yablonskaya, E. A. (1994). The Caspian Sea. SPB Academic Publishing.
- Kosarev, A. N., Tuzhilkin, V. S., & Kostianoy, A. G. (2004). Main features of the Caspian Sea hydrology. In Dying and dead seas climatic versus anthropic causes (pp. 159-184). Dordrecht: Springer Netherlands.
- Kostianoy, A. G., Ginzburg, A. I., Lebedev, S. A., Frankignoulle, M., & Delille, B. (2005). Fronts and mesoscale variability in the Caspian Sea. In A. G. Kostianoy & A. N. Kosarev (Eds.), The Caspian Sea Environment (pp. 135–179). Springer.
- Kourafalou, V. H., & Tsiaras, K. (2007). A nested circulation model of the North Aegean Sea. Ocean Science, 3(1), 1–16. https://doi.org/10.5194/os-3-1-2007
- Kurbanov, R., Murray, A., Yanina, T., & Buylaert, J. P. (2024). Dating the middle and late Quaternary Caspian Sea-level fluctuations: First luminescence data from the coast of Turkmenistan. Quaternary Geochronology, 83, 101599. https://doi.org/10.1016/j.quageo.2024.101599
- MacKinnon, J. A., Zhao, Z., Whalen, C. B., Waterhouse, A. F., Trossman, D. S., Sun, O. M., Goldbaum, D., Buijsman, M. C., Kunze, E., Brummel, N. M., & Alford, M. H. (2017). Climate process team on internal wave–driven ocean mixing. Bulletin of the American Meteorological Society, 98(11), 2429–2454. https://doi.org/10.1175/BAMS-D-16-0030.1
- Marshall, J., & Schott, F. (1999). Open-ocean convection: Observations, theory, and models. Reviews of Geophysics, 37(1), 1–64. https://doi.org/10.1029/98RG02739
- Mellor, G. L., & Yamada, T. (1982). Development of a turbulence closure model for geophysical fluid problems. Reviews of Geophysics, 20(4), 851–875. https://doi.org/10.1029/RG020i004p00851
- Nasrollahzadeh, H. S., Din, Z. B., Foong, S. Y., & Makhlough, A. (2008). Trophic status of the Iranian Caspian Sea based on water quality parameters and phytoplankton diversity. Continental Shelf Research, 28(9), 1153–1165. https://doi.org/10.1016/j.csr.2008.02.015
- Osborn, T. R. (1980). Estimates of the local rate of vertical diffusion from dissipation measurements. Journal of Physical Oceanography, 10(1), 83–89. https://doi.org/10.1175/1520-0485(1980)010<0083:EOTLRO>2.0.CO;2
- Özsoy, E., & Ünlüata, Ü. (1997). Oceanography of the Black Sea: A review of some recent results. Earth-Science Reviews, 42(4), 231–272. https://doi.org/10.1016/S0012-8252(97)81859-4
- Renssen, H., Lougheed, B. C., Aerts, J. C. J. H., De Moel, H., Ward, P. J., & Kwadijk, J. C. J. (2007). Simulating long-term Caspian Sea level changes: The impact of Holocene and future climate conditions. Earth and Planetary Science Letters, 261(3–4), 685–693. https://doi.org/10.1016/j.epsl.2007.07.037
- Rodionov, S. N. (1994). Global and regional climate interaction: The Caspian Sea experience. Springer.
- Sannino, G., Herrmann, M., Carillo, A., Rupolo, V., Ruggiero, V., Artale, V., & Heimbach, P. (2009). An

eddy-permitting model of the Mediterranean Sea with a two-way grid refinement at the Strait of Gibraltar. Ocean Modelling, 30(1), 56–72. https://doi.org/10.1016/j.ocemod.2009.06.002

- Stanev, E. V., & Peneva, E. L. (2002). Regional sea level response to global climatic change: Black Sea examples. Global and Planetary Change, 32(1–2), 33–47. https://doi.org/10.1016/S0921-8181(01)00148-5
- Stolberg, F., et al. (2013). Caspian Sea ecosystem profile. World Bank. https://documents.worldbank.org/en/publication/documents-reports/documentdetail/803551468262426883/caspian-sea-ecosystem-profile
- Sur, H. İ., Özsoy, E., & Ünlüata, Ü. (2000). Satellite-derived flow characteristics of the Caspian Sea. In A. G. Kostianoy & A. N. Kosarev (Eds.), The Caspian Sea Environment (pp. 109–134). Springer.
- Terziev, F. S., Kosarev, A. N., & Kerimov, A. A. (Eds.). (1992). Hydrometeorology and Hydrochemistry of the Seas, Vol. 6: The Caspian Sea, Issue 1. Hydrometeoizdat.
- Thomas, L. N., Tandon, A., & Mahadevan, A. (2008). Submesoscale processes and dynamics. In J. C. McWilliams & E. P. Chassignet (Eds.), Ocean Modeling in an Eddying Regime (pp. 17–38). American Geophysical Union. https://doi.org/10.1029/177GM04
- Thorpe, S. A. (2005). The turbulent ocean. Cambridge University Press.
- Tuzhilkin, V. S. (2005). Seasonal variability of the Caspian Sea thermohaline structure. In A. N. Kosarev & A. G. Kostianoy (Eds.), The Caspian Sea Environment (pp. 83–104). Springer.
- UNEP-DHI Centre. (2024). Caspian Sea fluctuations and climate change. UNEP-DHI Centre. https://unepdhi.org/wp-content/uploads/sites/2/2024/11/Caspian_Sea_working_paper.pdf
- Waterhouse, A. F., MacKinnon, J. A., Nash, J. D., Alford, M. H., Kunze, E., Simmons, H. L., Polzin, K. L., St. Laurent, L. C., Sun, O. M., Pinkel, R., Talley, L. D., Whalen, C. B., Carter, G. S., Fer, I., Waterman, S., Garabato, A. C. N., & Voet, G. (2014). Global patterns of diapycnal mixing from measurements of the turbulent dissipation rate. Journal of Physical Oceanography, 44(7), 1854–1872. https://doi.org/10.1175/JPO-D-13-0104.1
- Whalen, C. B., MacKinnon, J. A., Waterhouse, A. F., & Wunsch, C. (2020). Internal wave-driven mixing: Global patterns and trends. Annual Review of Marine Science, 12, 131–155. https://doi.org/10.1146/annurev-marine-010419-010935
- Wunsch, C., & Ferrari, R. (2004). Vertical mixing, energy, and the general circulation of the oceans. Annual Review of Fluid Mechanics, 36, 281–314. https://doi.org/10.1146/annurev.fluid.36.050802.122121
- Zavialov, P. O., Belokopytov, V. N., & Konovalov, B. V. (2003). Spreading of the river discharge plume of the Volga River in the Caspian Sea. Geophysical Research Letters, 30(12), 1630. https://doi.org/10.1029/2003GL017541
- Zonn, I. S., Kosarev, A. N., Glantz, M. H., & Kostianoy, A. G. (2010). The Caspian Sea Encyclopedia. Springer.